Longitudinal correlation of the triangular flow event plane in a hybrid approach with hadron and parton cascade initial conditions

Hannah Petersen, Vivek Bhattacharya, Steffen A. Bass, and Carsten Greiner

Longitudinal correlation of the triangular flow event plane in a hybrid approach with hadron and parton cascade initial conditions

Hannah Petersen, Vivek Bhattacharya, and Steffen A. Bass

Department of Physics, Duke University, Durham, North Carolina 27708-0305, United States

Carsten Greiner

Institut für theoretische Physik, Johann Wolfgang Goethe-Universität,
Max-von-Laue Strasse 1, D-60438 Frankfurt am Main, Germany

The longitudinal long-range correlations of the triangular flow event plane angles are calculated in a Boltzmann + hydrodynamics hybrid approach. The potential to disentangle different energy deposition scenarios is explored by utilizing two different transport approaches for the early non-equilibrium evolution. In the hadronic transport approach the particle production in high energy heavy ion reactions is mainly governed by string excitation and fragmentation processes which are absent in the parton cascade approach. We find that in both approaches the initial state shows a strong longitudinal correlation of the event plane angles which is diluted but still persists in the final state momentum space distributions of the produced particles. The observation of this effect is an important prerequisite for the experimental determination of odd harmonics that relies on a rapidity independent event plane definition.

Long- range rapidity correlations have been measured in heavy ion reactions at the Relativistic Heavy Ion Collider (RHIC) [1–5]. In two-particle correlations with a high p_T trigger hadron in the two-dimensional $\Delta\eta - \Delta\phi$ plane a ridge-like structure around $\Delta\phi = 0$ that extends over several units in pseudorapidity difference has been observed. Later on, the same phenomenon was also found in untriggered correlation functions and more detailed measurements with respect to particle composition and effective temperatures have been performed that indicate the 'bulk'-like properties of the ridge. Therefore, the original interpretation as a jet-medium effect [6–8] has been questioned and other explanations as e.g. Color-Glass-Condensate (CGC) inspired flux tube structures that get boosted by radial flow have become more favored [9–13].

Recently, initial state fluctuations have been proposed as the major source for many of the structures that appear in two-particle correlations [14–17]. Especially the third Fourier coefficient of the azimuthal distribution of the final state hadrons in momentum space, namely triangular flow, is studied with great interest [18–20]. This new flow observable is directly related to the fluctuations in the initial state and is absent in hydrodynamic calculations assuming smooth initial state profiles. Triangular flow is therefore independent of the collision centrality and very sensitive to the viscosity of the produced matter [21–24].

Even though a lot of progress has been made in the study of initial conditions, in particular regarding their fluctuations, it has been rather difficult to find an observable that is directly related to the mechanism of the initial energy deposition. Long-range rapidity correlations seem to be perfectly suited for this purpose, since they need to be build up very early during the evolution of the reaction due to causality. In order to study the effect of initial state fluctuations one needs to sim-

ulate the whole three-dimensional dynamical evolution event-by-event, which is computationally very expensive and makes it difficult to study two-dimensional 2-particle correlations in detail.

In this paper we propose a new observable that directly quantifies the longitudinal long-range correlation of triangular flow and explore it utilizing a state-of-the-art (3+1)d Boltzmann+hydrodynamics approach [25]. In [18] the pseudorapidity dependence of triangular flow in the hybrid approach has been published. The flatness over a broad range of pseudorapidities indicates long-range correlations, but does not actually prove that correlation. The preferred axis of the triangular shape could randomly fluctuate from one rapidity bin to the other and one would still observe a flat rapidity dependence as long as the magnitude of the third Fourier coefficient is the same in every bin. To really study the long-range correlation between the 'hot spots' we propose to investigate the triangular flow event plane in different rapidity bins separately and calculate the correlation between these and the overall event plane that is reconstructed from the full phase-space information. This observable has the great advantage that it is computationally less intensive than two-particle correlations and contains similar information.

In the following, we will explore this observable by using two different transport approaches to generate the initial conditions for the ideal hydrodynamic evolution to study its sensitivity to the energy deposition scenario. Let us first describe the two different approaches for the initial conditions in more detail. The initial conditions are either generated using hadron-string dynamics from the Ultra-relativistic Quantum Molecular Dynamics (UrQMD) approach [26, 27] or by using a parton cascade approach (PCM) [31, 33]. For the hadron-string dynamics, the initial binary nucleon-nucleon collisions are

modeled in UrQMD [26–28] following the Lund model of nucleon-nucleon reactions [29] involving color flux tubes excitation and fragmentation processes that provide long range rapidity correlations and fluctuations in the energy deposition in the transverse plane. The other option is to decompose the incoming nuclei according to parton distribution functions into quarks and gluons and use a parton cascade approach to simulate the early non-equilibrium evolution [30–33]. In this case, the cross-sections for 2→2 collisions and 1→2 splittings are given by perturbative QCD calculations. We have chosen this approach, since at first glance it does not contain any obvious mechanism to generate long-range correlations and thus provides a baseline to compare to. However, as we shall later see, the presence of radiated parton showers generated after the initial hard parton-parton scatterings is capable of generating long range rapidity correlations.
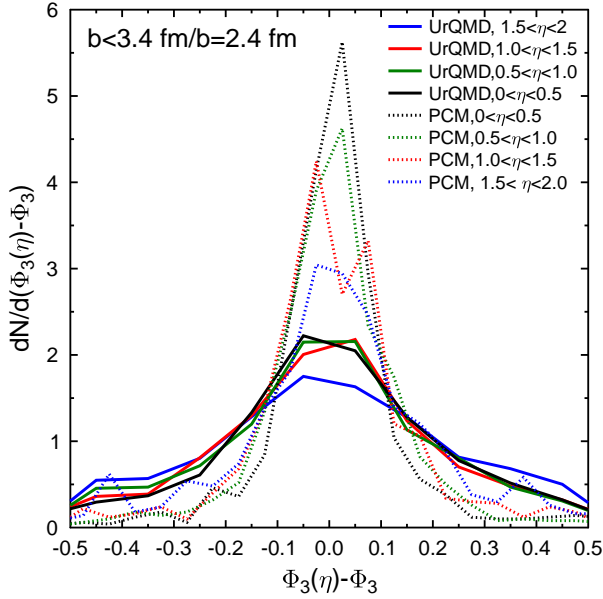

FIG. 1: (Color online) Distribution of the differences of the coordinate space event-plane angles Φ_3 in different rapidity slices in UrQMD (full line) and PCM (dotted line) initial conditions for central ($b < 3.4$ fm/$b = 2.4$ fm) Au+Au collisions at $\sqrt{s_{\rm NN}} = 200$ GeV.

For Au+Au collisions at the highest RHIC energies the starting time for the hydrodynamic evolution has been chosen to be $t_{\rm start} = 0.5$ fm in order to fit the final state pion multiplicity at midrapidity. Only the matter around midrapidity ($|y| < 2$) is considered to be locally thermalized and takes part in the ideal hydrodynamic evolution. To map the point particles from the hadron/parton cascade initial state to energy, momentum and net baryon density distributions each particle is represented by a three-dimensional Gaussian distribution [34]. The width of the Gaussian distribution has been chosen to be $\sigma = 1$
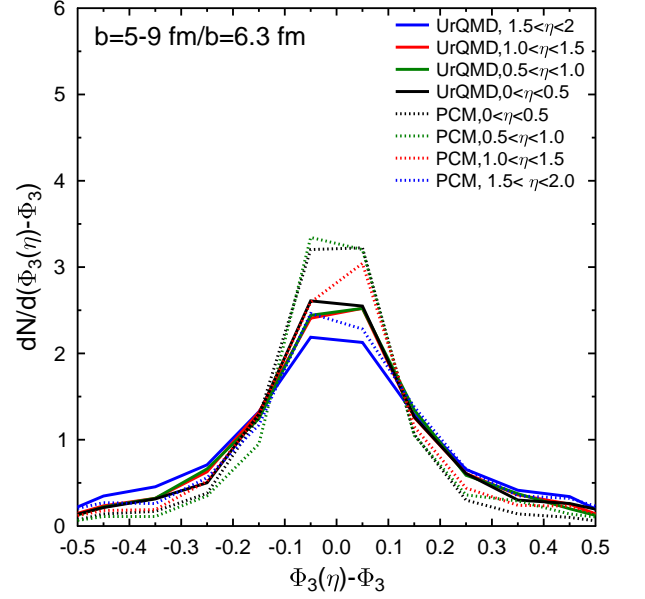

FIG. 2: (Color online) Distribution of the differences of the coordinate space event-plane angles Φ_3 in different rapidity slices in UrQMD (full line) and PCM (dotted line) initial conditions for mid-central ($b = 5 - 9$ fm/$b = 6.3$ fm) Au+Au collisions at $\sqrt{s_{\rm NN}} = 200$ GeV.

fm for UrQMD and $\sigma = 0.5$ fm for the PCM.

The ideal hydrodynamic evolution [35, 36] for the hot and dense stage of the collision translates the initial fluctuations in the transverse energy density to momentum space distributions. A hadron gas equation of state [37] has been used for the calculation with UrQMD initial conditions.

The transition from the hydrodynamic evolution to the transport approach when the matter is diluted in the late stage is treated as a gradual transition on an approximated constant proper time hyper-surface (see [38] for details). For the hadronic calculation an energy density of 713 MeV/fm^3 has been chosen as a transition criterion. Late stage hadronic rescattering and resonance decays are taken into account in the hadronic cascade.

The above event-by-event setup includes all the main ingredients that are necessary for the build up of triangular flow [18]. Since the complete final state particle distributions are calculated, an analysis similar to those applied by experimentalists is used.

In the initial state coordinate space distributions, one can define the event plane angles for different harmonics (we will concentrate on $n = 2$ and $n = 3$ in this analysis) in the following way:

$$\Phi_n = \frac{1}{n}\arctan\frac{\langle r^n \sin(n\phi)\rangle}{\langle r^n \cos(n\phi)\rangle} \qquad (1)$$

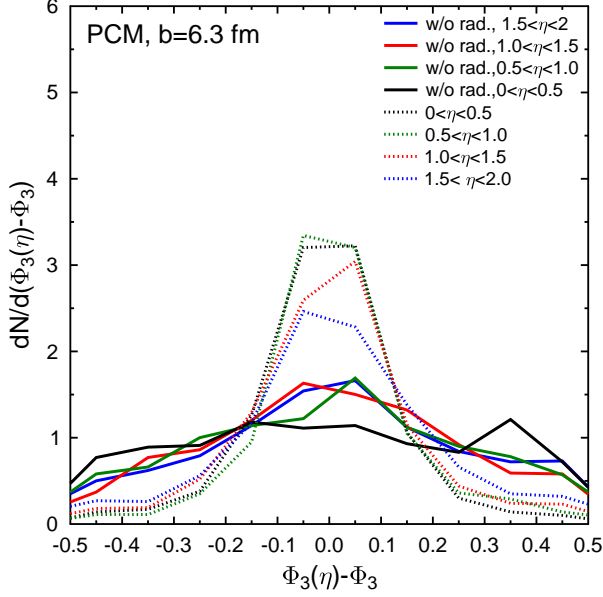where r and ϕ are the polar coordinates of the particles

FIG. 3: (Color online) Distribution of the differences of the coordinate space event-plane angles Φ_3 in different rapidity slices from the parton cascade in the default scenario (dotted line) and without gluon radiation (full line) initial conditions for mid-central ($b = 6.3$ fm) Au+Au collisions at $\sqrt{s_{\rm NN}} = 200$ GeV.
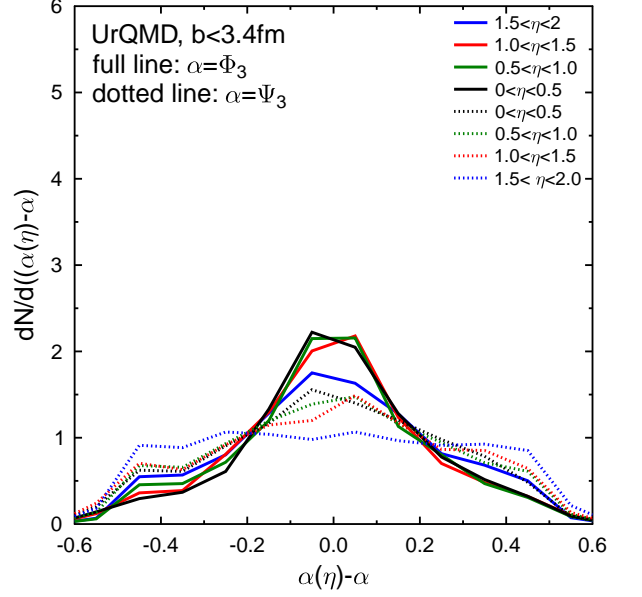
FIG. 4: (Color online) Distribution of the differences of the final momentum space (dotted line) vs initial coordinate space (full line) event-plane angles Φ_3 in different rapidity slices in the hybrid approach based on UrQMD initial conditions for central ($b < 3.4$ fm) Au+Au collisions at $\sqrt{s_{\rm NN}} = 200$ GeV.

in the center of mass frame of the collision. For elliptic flow this angle is the one that defines the so called participant plane. With the used conventions Φ_n is defined in the region between $-\pi/n$ and $+\pi/n$. To explore the longitudinal correlations, the event plane angle is calculated once in the whole rapidity range from $-2 < y < 2$ and then in different bins of width $|\Delta y| < 0.5$ separately. The distributions of the difference between those two angles in different rapidity slices is shown in Fig. 1. We have checked that the results are symmetric around midrapidity and the results are qualitatively unchanged if the bin size is varied from $|\Delta y| < 0.25 - 1.0$. Furthermore, the result without any additional physics mechanism that introduces a long-range correlation is a flat distribution (corresponding to a δ-function in the $\mathrm{d}N/\mathrm{d}\Delta y$ distribution) which we can reproduce by sampling particles from different events together and apply the exact same correlation analysis, similar to a mixed event technique. The rapidity range over which we performed our analysis corresponds to a maximum Δy of 4 units.

In Fig. 1 and 2 the correlation of the event plane angles is shown for two different centralities and the two different initial state transport approaches. In both cases, there is a strong correlation visible that is largest at midrapidity and smaller at the most forward y bin. In the parton cascade approach the longitudinal correlation can be attributed to the emission of parton showers that appear to be correlated to the preceding hard collision and

are emitted along the beam axis, whereas in the hadronic transport approach the string excitation and fragmentation mechanism offers the most plausible explanation.

Fig. 3 shows a comparison for the parton cascade initial conditions with and without time-like branchings, which initiate the parton showers. Without gluon emission after the hard collision, the longitudinal correlation of the triangular flow event plane angle in the initial state is much smaller (if existent at all). That proves that the initial long-range correlation in the parton cascade is mainly caused by this associated gluon radiation. Please note, that this finding is qualitatively different from the previously invoked jet-medium interactions that could lead to a ridge-like structure. The longitudinal correlations of the energy deposition in the parton cascade are generated before the medium is formed. The initial state features will then be further propagated in the hydrodynamic evolution. Therefore, the corresponding final state ridge structure would have the expected features, e.g. similar momentum distributions as the bulk particles.

To investigate if the initial long-range correlation survives the hydrodynamic expansion the same analysis can be performed for the final state momentum space event plane angles,

$$\Psi_n = \frac{1}{n} \arctan \frac{\langle p_T \sin(n\phi_p) \rangle}{\langle p_T \cos(n\phi_p) \rangle} \quad , \qquad (2)$$
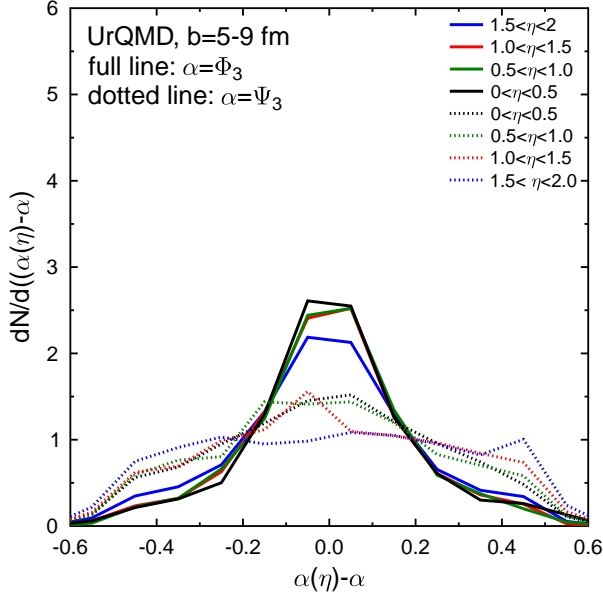
FIG. 5: (Color online) Distribution of the differences of the final momentum space (dotted line) vs coordinate space (full line) event-plane angles Φ_3 in different rapidity slices in the hybrid approach based on UrQMD initial conditions for mid-central ($b = 5 - 9$ fm) Au+Au collisions at $\sqrt{s_{NN}} = 200$ GeV.
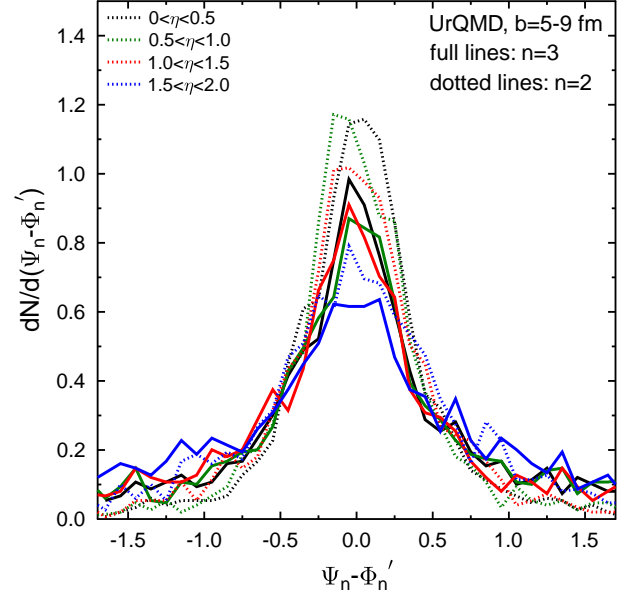
FIG. 6: (Color online) Event-by-event correlation between initial and final state event plane angles for elliptic (dotted line) and triangular flow (full line) in different rapidity slices in the hybrid approach based on UrQMD initial conditions for mid-central ($b = 5 - 9$ fm) Au+Au collisions at $\sqrt{s_{NN}} = 200$ GeV.

where (p_T, ϕ_p) are polar coordinates in momentum space. In Figs. 4 and 5 the longitudinal correlation of the final state event plane angles Ψ_3 is shown in comparison to the previously presented distribution for Φ_3. The correlation gets significantly diluted during the ideal hydrodynamic expansion, but it persists also in the final state particle distribution with the exception of the most forward/backward rapidity bin that is accessible in this calculation. We have checked that the same result qualitatively is obtained by employing the parton cascade initial conditions. The final state event plane angles Ψ_3 in different rapidity bins could be measured in experiment to investigate the longitudinal correlations of triangular flow and to legitimate the assumption that the event plane angle does not change as a function of rapidity.

Another way to study the initial and final state correlation of the event plane angles is shown in Fig. 6. Here, the differences between the two angles in different rapidity bins are shown for mid-central collisions in the hybrid approach based on UrQMD initial conditions. As a comparison the correlation for elliptic flow at is also shown. For the three rapidity bins between 0 and 1.5 the correlation is clearly visible for triangular flow as well, whereas it is less pronounced in the most forward/backward bin. This confirms the conclusion of the Fig. 5 that the long-range correlation only survives over three units in rapidity around $y = 0$.

In summary, we have proposed a new way to investigate the long-range correlations of triangular flow in heavy ion collisions. A hadron and a parton cascade approach both lead to sizable long-range correlation in the initial state. These correlations are translated to the final state hadron distributions, but are significantly diluted and smoothed out during the final hadronic rescattering. Measuring the triangular flow event plane angles in different rapidity bins serves as a pre-requisite to legitimate the assumption of a constant event plane over rapidity as it is commonly assumed by experimental groups. The second conclusion is that one needs to take into account a realistic dynamical evolution (e.g. [39, 40]) to prove that the long-range correlations that might be initially established also survive to the final state particle distributions instead of simple parametrizations.

[1] J. Adams *et al.* [STAR Collaboration], particles in pp and Au + Au collisions at s(NN)**(1/2) = 200-GeV," Phys. Rev. Lett. **95**, 152301 (2005). [nucl-ex/0501016].

[2] J. Adams *et al.* [STAR Collaboration], Phys. Rev. C **73**, 064907 (2006) [arXiv:nucl-ex/0411003].

[3] J. Putschke, J. Phys. G **34**, S679 (2007) [arXiv:nucl-ex/0701074].

[4] B. I. Abelev *et al.* [STAR Collaboration], Phys. Rev. C **80**, 064912 (2009) [arXiv:0909.0191 [nucl-ex]].

[5] B. Alver *et al.* [PHOBOS Collaboration], Phys. Rev. Lett. **104**, 062301 (2010) [arXiv:0903.2811 [nucl-ex]].

[6] A. Majumder, B. Muller and S. A. Bass, Phys. Rev. Lett. **99**, 042301 (2007) [arXiv:hep-ph/0611135].

[7] E. V. Shuryak, Phys. Rev. C **76**, 047901 (2007) [arXiv:0706.3531 [nucl-th]].

[8] C. Y. Wong, Phys. Rev. C **78**, 064905 (2008) [arXiv:0806.2154 [hep-ph]].

[9] A. Dumitru, F. Gelis, L. McLerran and R. Venugopalan, Nucl. Phys. A **810**, 91 (2008) [arXiv:0804.3858 [hep-ph]].

[10] S. Gavin, L. McLerran and G. Moschelli, Phys. Rev. C **79**, 051902 (2009) [arXiv:0806.4718 [nucl-th]].

[11] K. Dusling, F. Gelis, T. Lappi and R. Venugopalan, Nucl. Phys. A **836**, 159 (2010) [arXiv:0911.2720 [hep-ph]].

[12] G. Moschelli and S. Gavin, Nucl. Phys. A **836**, 43 (2010) [arXiv:0910.3590 [nucl-th]].

[13] G. Moschelli and S. Gavin, arXiv:0911.0094 [nucl-th].

[14] B. Alver and G. Roland, Phys. Rev. C **81**, 054905 (2010) [Erratum-ibid. C **82**, 039903 (2010)] [arXiv:1003.0194 [nucl-th]].

[15] M. Luzum, Phys. Lett. B **696**, 499 (2011) [arXiv:1011.5773 [nucl-th]].

[16] Y. Hama, R. P. G. Andrade, F. Grassi and W. L. Qian, Nonlin. Phenom. Complex Syst. **12**, 466 (2009) [arXiv:0911.0811 [hep-ph]].

[17] P. Sorensen, B. Bolliet, A. Mocsy, Y. Pandit and N. Pruthi, arXiv:1102.1403 [nucl-th].

[18] H. Petersen, G. Y. Qin, S. A. Bass and B. Muller, Phys. Rev. C **82**, 041901 (2010) [arXiv:1008.0625 [nucl-th]].

[19] G. Y. Qin, H. Petersen, S. A. Bass and B. Muller, Phys. Rev. C **82**, 064903 (2010) [arXiv:1009.1847 [nucl-th]].

[20] G. L. Ma and X. N. Wang, arXiv:1011.5249 [nucl-th].

[21] B. H. Alver, C. Gombeaud, M. Luzum and J. Y. Ollitrault, Phys. Rev. C **82**, 034913 (2010) [arXiv:1007.5469 [nucl-th]].

[22] B. Schenke, S. Jeon and C. Gale, Phys. Rev. Lett. **106**, 042301 (2011) [arXiv:1009.3244 [hep-ph]].

[23] B. Schenke, S. Jeon and C. Gale, arXiv:1102.0575 [hep-ph].

[24] D. Teaney and L. Yan, arXiv:1010.1876 [nucl-th].

[25] H. Petersen, J. Steinheimer, G. Burau, M. Bleicher and H. Stocker, Phys. Rev. C **78**, 044901 (2008) [arXiv:0806.1695 [nucl-th]].

[26] S. A. Bass *et al.*, Prog. Part. Nucl. Phys. **41**, 255 (1998) [Prog. Part. Nucl. Phys. **41**, 225 (1998)] [arXiv:nucl-th/9803035].

[27] M. Bleicher *et al.*, J. Phys. G **25**, 1859 (1999) [arXiv:hep-ph/9909407].

[28] H. Petersen, M. Bleicher, S. A. Bass and H. Stocker, arXiv:0805.0567 [hep-ph].

[29] B. Andersson, G. Gustafson, G. Ingelman and T. Sjostrand, Phys. Rept. **97**, 31 (1983).

[30] K. Geiger and B. Muller, Nucl. Phys. B **369**, 600 (1992).

[31] K. Geiger, Phys. Rept. **258**, 237 (1995).

[32] K. Geiger, Comput. Phys. Commun. **104**, 70 (1997) [arXiv:hep-ph/9701226].

[33] S. A. Bass, B. Muller and D. K. Srivastava, Phys. Lett. B **551**, 277 (2003) [arXiv:nucl-th/0207042].

[34] J. Steinheimer, M. Bleicher, H. Petersen, S. Schramm, H. Stocker and D. Zschiesche, Phys. Rev. C **77**, 034901 (2008) [arXiv:0710.0332 [nucl-th]].

[35] D. H. Rischke, S. Bernard and J. A. Maruhn, Nucl. Phys. A **595**, 346 (1995) [arXiv:nucl-th/9504018].

[36] D. H. Rischke, Y. Pursun and J. A. Maruhn, Nucl. Phys. A **595**, 383 (1995) [Erratum-ibid. A **596**, 717 (1996)] [arXiv:nucl-th/9504021].

[37] D. Zschiesche, S. Schramm, J. Schaffner-Bielich, H. Stoecker and W. Greiner, Phys. Lett. B **547**, 7 (2002) [arXiv:nucl-th/0209022].

[38] Q. f. Li, J. Steinheimer, H. Petersen, M. Bleicher and H. Stocker, Phys. Lett. B **674**, 111 (2009) [arXiv:0812.0375 [nucl-th]].

[39] Z. Xu, C. Greiner, including three-body interactions in a parton cascade," Phys. Rev. **C71**, 064901 (2005). [hep-ph/0406278].

[40] Z. Xu, C. Greiner, ultrarelativistic heavy-ion collisions," Phys. Rev. **C76**, 024911 (2007). [hep-ph/0703233].